# Effect of Metal Binding on Electrogenic Proton Transfer Associated with Reduction of the Secondary Electron Acceptor ($Q_B$) in *Rhodobacter sphaeroides* Chromatophores†

Sonia Keller,‡ J. Thomas Beatty,§ Mark Paddock,⊥ Jacques Breton,‡ and Winfried Leibl*,‡

*CEA Saclay, Section de Bioénergétique, 91191 Gif-sur-Yvette, France, Department of Microbiology and Immunology, University of British Columbia, Vancouver, Canada, and Department of Physics, University of California, San Diego, La Jolla, California 92093*

*Received June 5, 2000; Revised Manuscript Received October 30, 2000*

ABSTRACT: The influence of metal ion ($Cd^{2+}$, $Zn^{2+}$, $Ni^{2+}$) binding on the electrogenic phases of proton transfer connected with reduction of quinone $Q_B$ in chromatophores from *Rhodobacter sphaeroides* was studied by time-resolved electric potential changes. In the presence of metals, the electrogenic transients associated with proton transfer on first and second flash at pH 8 were found to be slower by factors of 3−6. This is essentially the same effect of metal binding that was observed on optical transients in isolated reaction centers (RC), where the metal ion was shown to inhibit proton transfer [Paddock, M. L., Graige, M. S., Feher, G., and Okamura, M. Y. (1999) *Proc. Natl. Acad. Sci. U.S.A. 96,* 6183−6188]. The effect of metal binding on the kinetics in chromatophores is, therefore, similarly attributed to inhibition of proton uptake, which becomes rate-limiting. A striking observation was an increase in the amplitude of the electrogenic proton-uptake phase after the first flash with bound metal ion. We attribute this to a loss of internal proton rearrangement, requiring that the protons that stabilize $Q_B^-$ come from solution. In mutant RCs, in which His-H126 and His-H128 are replaced with Ala, the apparent binding of $Cd^{2+}$ and $Ni^{2+}$ was decreased, showing that the binding site of these metal ions is the same as found in RC crystals [Axelrod, H. L., Abresch, E. C., Paddock, M. L., Okamura, M. Y., and Feher, G. (2000) *Proc. Natl. Acad. Sci. U.S.A. 97,* 1542−1547]. Therefore, the unique proton entry point near His-H126, His-H128, and Asp-M17 that was identified in isolated RCs is also the entry point in chromatophores.

Photosynthetic reaction centers (RC)[1] are integral membrane protein complexes that catalyze the conversion of light energy into electrochemical energy. Two families of RCs can be distinguished according to the nature of their terminal electron acceptor complex, which consists either of low-potential iron−sulfur centers (type I RCs) or a quinone-iron acceptor complex (type II RCs). The functional feature common to all types of RCs is ultrafast light-induced primary charge separation followed by vectorial electron transfer along a chain of cofactors. In type II RCs, the quinone-iron acceptor complex has a special function insofar as it works as a two-electron gate. A loosely bound secondary quinone acceptor, $Q_B$, accepts successively two electrons from the firmly bound primary quinone acceptor $Q_A$, as well as two protons from solution before leaving its binding site. This bioenergetically important mechanism of coupling of electron transfer and proton transfer has been the subject of numerous studies (for reviews see refs *1* and *2*). The best-characterized system is the RC of the purple bacterium *Rhodobacter sphaeroides*. Because of the availability of detailed structural models based on X-ray crystallography, as well as site-directed mutants, a large amount of structural and functional information is available (see ref *3* for reviews).

In isolated RCs from *Rb. sphaeroides*, formation of $Q_A^-$ or $Q_B^-$ leads to substoichiometric proton uptake (*4*, *5*). It is widely accepted that this proton uptake is due to p*K* shifts of amino acids induced by electrostatic interaction with the negative charge on the quinones but that the semiquinone forms of $Q_A$ and $Q_B$ are not protonated at physiological pH. The transfer of the first electron to $Q_B$ shows little pH dependence at neutral pH values (*6*). At high pH, where the free energy difference between the states $Q_A^-Q_B$ and $Q_AQ_B^-$ becomes small, the electron transfer becomes strongly pH-dependent. In contrast, the transfer of the second electron is strongly coupled to the transfer of a proton forming the state $Q_BH^-$ and displays a stronger pH dependence near neutral pH values (*7*). Studies of the dependence of the rate of the reaction on the driving force for electron transfer from $Q_A^-$ to $Q_B^-$ elucidated the mechanism of this protonation-coupled electron-transfer reaction (*8*, *9*). It was concluded that energetically unfavorable protonation of $Q_B^-$ precedes rate-

† This work was supported by grants to M.P. (NSF MCB94-16652, NIH GM 41637, and GM 13191). J.T.B. was supported by a grant from the Canadian CIHR.

* To whom correspondence should be sent. W. Leibl, CEA Saclay, Section de Bioénergétique, Bât. 532, 91191 Gif-sur-Yvette, France. Phone: (331)69085289. Fax: (331)69088717. E-mail: Leibl@dsvidf.cea.fr.

‡ CEA Saclay.

§ University of British Columbia.

⊥ University of California.

[1] Abbreviations: reaction centers (RC); EDTA, ethylenediaminetetraacetic acid; MES, 2-[*N*-morpholino]ethanesulfonic acid; OM, *n*-octadecyl mercaptan; PMS, phenazine methosulfate; P, primary electron donor; $Q_A$, $Q_B$, primary, secondary quinone acceptor; *Rb.*, *Rhodobacter*; RC, reaction center; TMPD, *N*,*N*,*N*′,*N*′-tetramethyl-*p*-phenylenediamine.

10.1021/bi001286n CCC: $20.00 
Published on Web 12/15/2000

limiting electron transfer. Formation of $Q_BH^-$ then triggers the transfer of the second proton to form the neutral dihydroquinone, which leaves the $Q_B$ binding site and is replaced by an oxidized quinone from the pool. In isolated RCs, the transfer of the first and second proton to reduced $Q_B$ cannot be kinetically separated, and virtually all of the proton supply to $Q_B$ appears with the kinetics of the second electron transfer.

The transfer of the protons through the protein matrix is thought to rely on the presence of a connected network of protonatable amino acid residues or water molecules (*10*). On the basis of site-directed mutagenesis, several residues in the vicinity of $Q_B$ have been identified as crucial for efficient proton transfer. These residues include Ser L223, Asp L213, and Glu L212. Replacement of any of these residues with a nonprotonatable residue leads to dramatic reduction in the rate of transfer of the first or second proton (*11*−*13*). High-resolution X-ray crystallography has revealed the existence of three possible proton pathways connecting the cytoplasmic surface of the protein to these key residues (*14*, *15*). All paths consist of a chain of protonatable groups (i.e., protonatable amino acid side chains or water molecules). They have different lengths and distinct entry points for the protons. Following the finding of $Zn^{2+}$ binding to the RC surface (*16*), the predominance of one of these pathways for the first protonation of $Q_B^-$ was shown by a ∼10-fold decrease in the rate of proton transfer upon binding of a single $Zn^{2+}$ or $Cd^{2+}$ ion to the RC surface (*17*). The binding site for $Cd^{2+}$ and $Zn^{2+}$ was identified by X-ray diffraction to involve two histidine residues (His-H126, His-H128) as well as an aspartic acid residue (Asp-H124) on the cytoplasmic surface of subunit H near one of the previously proposed pathways (*14*, *18*).

All three possible pathways also connect the surface to a cluster of strongly coupled acids near $Q_B$ composed of Asp-L213, Asp-L210, Asp-M17, Glu-H173, Asp-H170, and Asp-H124 (*14*). The functional importance of groups within this cluster has been demonstrated by numerous experimental data including kinetics and stoichiometry of proton uptake, kinetics of electron transfer, as well as the equilibrium between the states $Q_A^-Q_B$ and $Q_AQ_B^-$ (*19*, *20*). In addition, the strong electrostatic interaction between these protonatable residues gives rise to some unique properties, including nonclassic titration behavior (*21*−*23*); such behavior has been observed for Glu-L212 (*24*, *25*). The cluster may prepare the electrostatic environment for efficient electron and proton transfer to $Q_B$ or serve as an internal proton reservoir.

The interesting question arises whether the scenario described in isolated RC (metal binding blocking a unique entry point for protons to $Q_B$) also applies to membrane-bound RCs, i.e., RCs in chromatophores. In fact, several experimental observations indicate significant differences between detergent-solubilized RCs and chromatophores with respect to the function of the quinone acceptor complex. $Q_A^-Q_B \rightarrow Q_AQ_B^-$ electron transfer was found to be dependent on the state of purification for isolated RCs and significantly faster in chromatophores (*26*, *27*). Furthermore, evidence for a protonation of the semiquinone state of $Q_B$ has been reported in chromatophores, indicating a higher p*K* of the semiquinone in chromatophores as compared to isolated RCs (*28*). These differences between isolated and membrane-bound RCs might have their origin in a modified binding of $Q_B$. The importance of protein-quinone coupling as a variable but controlling feature of electron transfer has been pointed out by Tiede et al. (*29*). In *Rhodopseudomonas viridis*, different positions of the quinone ring were determined for ubiquinones with different isoprenoid tail lengths (*30*). Only the first three isoprenoid units interact with the RC protein (*31*). The rest of the tail is found in the surrounding detergent molecules. In the membrane, it is likely that interactions exist between the hydrophobic tail of the quinone and other proteins that surround the RC. In particular, the PufX protein was shown to facilitate access of quinones to the $Q_B$ site through the surrounding antenna complex (*32*). It has been pointed out that this function requires specific interactions between PufX, antenna proteins, quinones, and the RC $Q_B$ site (*33*).

In isolated RCs, electron and proton transfer to $Q_B$ have been studied by several methods including kinetic absorption change, proton uptake, and photovoltage. For the more native system of RCs embedded in their membrane environment optical and proton uptake measurements are very difficult to make and even harder to interpret, whereas the technique of photovoltage measurements is particularly suited for these investigations. On the basis of direct, flash-induced time-resolved electrometric detection of the membrane potential, this technique provides information on the rates of electrogenic electron and proton-transfer reactions as well as the relative transmembrane distances between the donor and the acceptor molecules involved in these transfers. Whereas the kinetic information obtainable from electrogenicity, proton uptake, and absorption change measurements should be equivalent (see, for example, ref *34* for a comparative study in proteoliposomes), the information about the transmembrane distance of charge movement is a specific feature of electrogenicity measurements, not accessible by the other methods.

Previous photoelectric studies have shown that electron transfer from $Q_A^-$ to $Q_B$ is not detected directly due to the small electrogenicity of this reaction (see ref *35* for a review). This agrees well with the two quinones having similar transmembrane positions. In contrast, proton-transfer coupled with the reduction of $Q_B$ gives rise to characteristic electrogenic phases in the microsecond-to-millisecond time range, since the proton-transfer event involves (partial) transmembrane charge movement.

In this work, we use time-resolved photovoltage measurements to study electrogenic proton transfer to $Q_B$ in RCs embedded in their native membrane environment. The effects of binding of different metal ions ($Zn^{2+}$, $Cd^{2+}$, $Ni^{2+}$) as well as of mutation of two histidine residues proposed as the entry points for proton uptake were investigated, to test whether the model of a unique proton-transfer pathway emerging from observations on isolated RCs also applies to the case of the RC in situ. In addition, we address the mechanism by which metal binding perturbs the function of the quinone acceptor complex.

## EXPERIMENTAL PROCEDURES

*Sample Preparation.* Cells of *Rb. sphaeroides* R26 were grown anaerobically in Hutner media and stored at −20 °C until use. The 2× histidine mutant [HA(H126)/HA(H128)] was constructed by use of the QuickChange PCR mutagen-

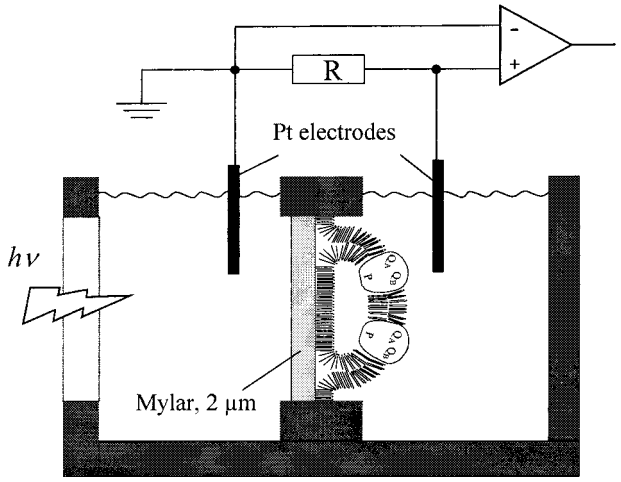


FIGURE 1: Schematic drawing of the experimental setup. A lipid-coated Mylar film (2 $\mu$m) separates two aqueous compartments in which the two platinum electrodes are immersed. Fusion of chromatophores is thought to form multiple small "blisters" on the supporting film (*48*). The original asymmetry of the RCs is preserved with the donor side inside the vesicles. Vectorial charge transfer within the RC leads to variation in the membrane potential that is capacitatively transferred through the supporting film. The electrodes are connected to an electrometer amplifier resulting in a current-clamped detection system.

esis kit (Stratagene) with adherence to the manufacturer's instructions and a template consisting of a 1.3 kilobase *Bam*HI fragment containing the *Rb. sphaeroides puhA* gene (*36*) inserted into the plasmid pTZ18. DNA sequencing of the entire region between the *Apa*I and *Bgl*I sites confirmed the mutations. The mutant *Apa*I−*Bgl*I fragment was combined with the remainder of the *puhA* gene and cloned into a pRK415 (*37*) derivative that contains the *Rb. sphaeroides puc* promoter (*38*) for expression of the H subunit. This construct was introduced into strain ΔPUHA (*39*). Cells were grown semi-aerobically, and chromatophores were prepared by French-press treatment as described in ref *40* and purified by sucrose gradient. The purified chromatophores were not frozen but kept on ice and used within a few days after preparation.

*Photovoltage Measurements*. A supported membrane system was created by fusion of chromatophores to a lipid-impregnated support similarly as described (*41*, *42*). The support was either a Mylar film (Goodfellow, thickness 2 $\mu$m) separating two aqueous compartments (see Figure 1) or a planar gold electrode treated with *n*-octadecyl mercaptan (OM, Sigma) to form a self-assembled hydrophobic layer. The latter configuration consisted of only one aqueous compartment. The results obtained with the two types of supports were identical, but the much higher capacitance of the gold/OM system in principle allows monitoring fusion of chromatophores by capacitance measurements (Keller et al., unpublished results). The lipid for impregnation was a mixture of 1.2% (wt/v) L-1,2-diphytanoyl-3-phosphatidylcholine (Avanti Polar Lipids, Birmingham, USA) and 0.025% (wt/v) octadecylamine (Sigma) in *n*-decane (Merck). Before use, the deposited lipid solution was dried for about 3 h to remove most of the solvent. Fusion of chromatophore vesicles to the lipid layer was induced by addition of 20 mM $CaCl_2$. After incubation for about 1 h, the chromatophore suspension was replaced by an electrolyte solution containing 100 mM KCl and buffer and redox chemicals as indicated. Buffers and redox chemicals were chosen that did not react with the metal ions (see below).

Potential changes were detected via two electrodes consisting of two platinum wires for the configuration with two compartments separated by the film or consisting of one platinum wire and the planar gold electrode for the second configuration, respectively. The electrodes were connected to the input of an electrometer-amplifier (input impedance $>10^{14}$ Ω, bandwidth DC-10 MHz) and subsequently amplified by a low noise preamplifier (Stanford Research Systems, model SR560, bandwidth 1 MHz). Traces were recorded without averaging on a digital storage oscilloscope (TDS 744A, Tektronix) and in parallel on a data acquisition system of local design offering a quasi-logarithmic time base. A Faraday cage shielded the cell and the electrometer amplifier. Excitation was with one flash or a series of two saturating flashes from a Q-switched, frequency-doubled Nd:YAG laser (Quantel, France, fwhm 7 ns, $\lambda = 532$ nm, energy ~20 mJ). All experiments were performed at 25 °C.

The kinetic analysis was performed with a nonlinear least-squares curve-fitting program (Microcal Origin). It was important to include the decay of the signals in the fit of the kinetics. Traces recorded on the second flash were not corrected for the baseline drift induced by the tail of the preceding signal of the first flash (fired 500 ms before the second flash). This drift is negligible for short times (<100 ms) and does not affect the result of the kinetic analysis.

The method of fusion of membrane vesicles to a lipid layer is known to induce partial depletion of quinones from the membrane and the $Q_B$ site (*43*). The procedure used here was found to result in about 60−80% $Q_B$ occupancy as measured by the relative amplitude of the second flash in the presence of an efficient external electron donor. In principle, the occupancy of the $Q_B$ site can be increased by addition of excess ubiquinone, either to the lipid mixture (ubiquinone-10) or to the electrolyte solution (ubiquinone-2). However, reconstitution with ubiquinone-10 is not very efficient [a ratio of 100 ubiquinone-10/RC results in reconstitution of >90% (*44*)], and addition of ubiquinone-2 may introduce heterogeneity either due to a binding site different from the native quinone (*30*) or due to slightly modified energetic parameters (*45*). In view of the fair amount of $Q_B$ preserved by our fusion procedure for the measurements presented here, such a reconstitution of full $Q_B$ occupancy was not applied. As a consequence of incomplete occupancy of the $Q_B$ site, the total amplitude on the second flash is proportionally reduced due to the presence of $Q_A^-$ in the minor fraction of RCs containing no $Q_B$. This neither affects the relative amplitude nor the kinetics of proton-transfer phases on the second flash. However, the relative amplitude of proton-transfer phases related to $Q_B$ reduction on the first flash may be underestimated. To exclude interference by variation of $Q_B$ occupancy, the same sample was used for measuring the photovoltage response in the absence and presence of metal ions. The orientation of the majority of RCs with respect to the support can be deduced from the polarity of the photovoltage signal. It was such that the acceptor side was exposed to the electrolyte/buffer solution and the donor side faced the support. This orientation is ideal to study exchange of protons between the acceptor side and the solution. The degree of orientation was verified by control experiments comparing the photovoltage amplitudes induced

Scheme 1: Schematic Representation of Charge Transfer Reactions Contributing to the Electrogenicity Detected on the First and the Second Flash[a]

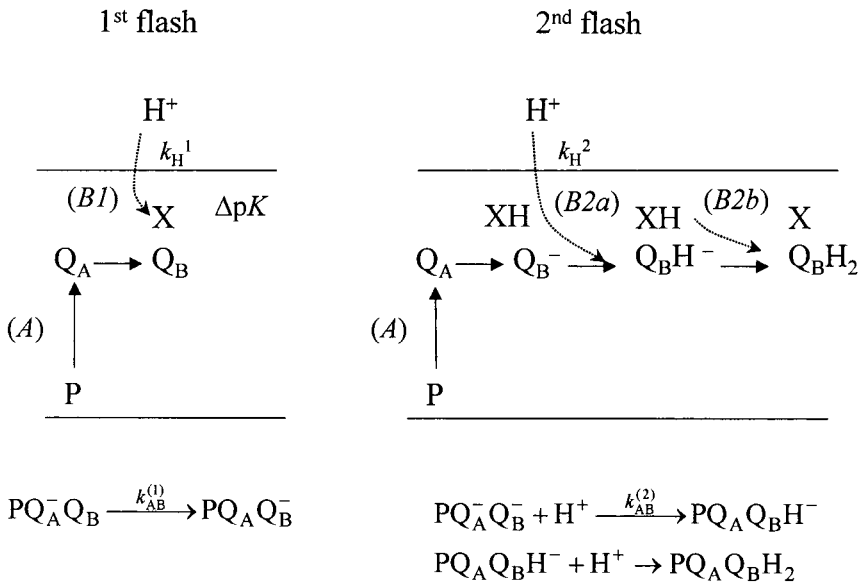


[a] It is assumed that after each flash the oxidized primary donor is re-reduced rapidly by a fast donor. *A* is the dominant electrogenic phase due to electron transfer from P to $Q_A$. *B1* and *B2* (*B2* = *B2a* + *B2*b) are electrogenic phases attributed to all proton-transfer reactions connected with the first and second reduction of $Q_B$, respectively. X represents one or more residues the p*K* of which is shifted by Δp*K* upon formation of $Q_B^-$ leading to substoichiometric proton uptake (*B1*). Phase *B2a* represents transfer of one proton to singly reduced $Q_B$ followed by transfer of the second electron. Phase *B2b* corresponds to second protonation of the doubly reduced $Q_B$. The latter, internal proton transfer is presumably fast and phases *B2a* and *B2b* can be kinetically separated only at lower temperatures (*54*). The sum of the amplitudes of phase *B1* and *B2* corresponds to the transfer of two protons from solution to $Q_B$. Because of the relatively high effective dielectric constant of the region between $Q_B$ and the cytoplasmic surface, for a given transmembrane distance the proton-transfer steps are expected to be less electrogenic than electron transfer from P to $Q_A$, the latter occurring in a region of the membrane protein with lower effective dielectric constant.

by the first and the second flash in the presence of the $Q_B$ inhibitor terbutryn and after addition of the membrane-impermeable electron donor cytochrome *c* and was found to be close to 100% (not shown). The samples were preadapted in the dark for 5 min before excitation, which was sufficient to ensure that $Q_B$ was in the oxidized form before the flash sequence. No signal averaging was applied.

Control experiments were performed to verify that contributions to the photovoltage signal from electrogenic reactions other than the proton transfer phases under study were either absent or kinetically separated. Potential contributions can be expected from reduction of $P^+$ by external donors (*46*) and from electrogenic reactions within the $bc_1$ complex related to quinol oxidation (*47*). Concerning reduction of $P^+$, it was not possible to use external donor and mediator combinations typically employed, like ferrocyanide and *N*,*N*,*N*′,*N*′-tetramethyl-*p*-phenylenediamine (TMPD), as this leads to formation of a precipitate when the metal ions are added. Instead, we found that ascorbate/phenazine-methosulfate (PMS) is a suitable donor/mediator couple, compatible with $Cd^{2+}$, $Zn^{2+}$, and $Ni^{2+}$. The rate of $P^+$ reduction was tested by absorption change measurements in solution to occur in about 20 ms (1 mM sodium ascorbate, 2 μM PMS, pH 8). This is slow enough to avoid interference with the proton-transfer phases. Concerning a potential contribution from quinol oxidation by the $bc_1$ complex, it can be detected under suitable conditions as a further electrogenic phase after the second flash in the 10−100 ms time range. We verified that addition of specific inhibitors of this reaction (antimycin and myxothiazol) had no effect on the photovoltage response under our conditions (not shown). The reason for the absence of phases connected with the reoxidation of quinol in the $bc_1$ complex is probably the relatively low redox potential in the experiments presented here. Another reason might be because quinone diffusion in the small "blisters" formed by fusion of the chromatophores (*48*) is restricted.

*Photovoltage Nomenclature.* Flash excitation of chromatophores fused with a lipid layer on a solid support gives rise to a photovoltage signal, which in general shows several kinetic phases (Scheme 1). We shall use the nomenclature introduced by Drachev et al. (*49*) to describe the electrogenic signals. The unresolved electrogenic phase due to $P^+Q_A^-$ formation is denoted as phase A and the additional slower electrogenic phase attributable to proton transfer related to $Q_B$ function induced by the first and second flash as phase B1 and B2, respectively.

The dominant electrogenic phase (A) on the first as well as on the second flash is a fast change of the membrane potential due to electron transfer from the primary donor P to the primary quinone acceptor $Q_A$. This charge separation occurs in two consecutive electrogenic steps with time constants of about 50 ps (trapping limited) and 200 ps (*50*) and is not time-resolved in this experiment. The following step of electron transfer from $Q_A^-$ to the secondary quinone acceptor $Q_B$ is not electrogenic and does not contribute to the photovoltage signal. However, proton-transfer events related to the reduction of $Q_B$ have been shown to result in characteristic photovoltage phases with kinetics in the 100 μs time range (*49*, *51*−*54*). The electrogenic phases B1 and B2 can be attributed to substoichiometric proton uptake due to protonation of amino acid residues near $Q_B$ and transfer of two protons to $Q_B^-$ to form the ubiquinol $Q_BH_2$, after the first and the second flash, respectively. In the presence of

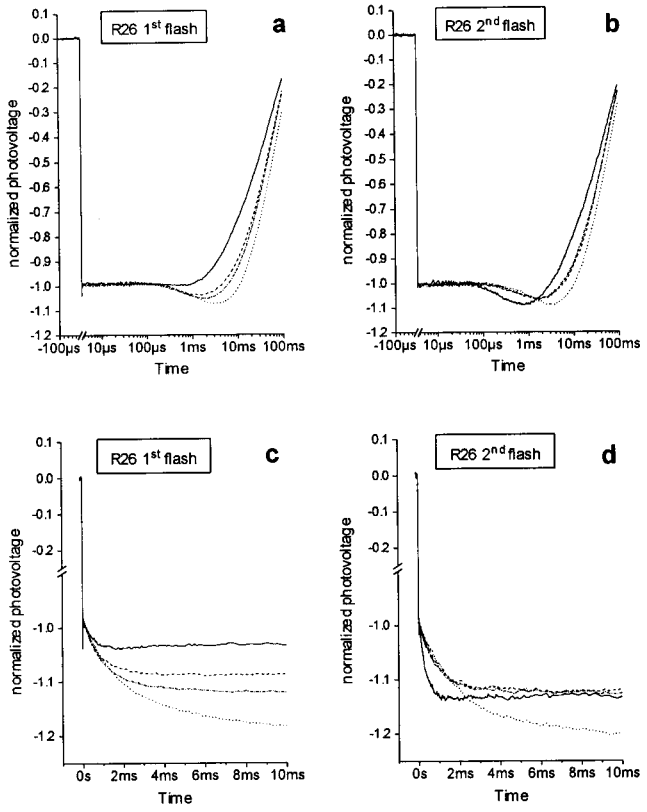


FIGURE 2: Effect of metal binding on photovoltage transients in chromatophores from *Rb. sphaeroides* R26. (Panels a and c) first flash; (panels b and d) second flash of the same series of two flashes spaced 0.5 s. (—) no addition, (- - -) 100 $\mu$M $Cd^{2+}$, (•••) 100 $\mu$M $Zn^{2+}$, (•-•-•-) 100 $\mu$M $Ni^{2+}$. 10 mM Hepes pH 8, 100 mM KCl, 1 mM ascorbate, and 2 $\mu$M PMS were present in all samples. The same sample of chromatophores fused to a Mylar film was used for all experiments. Initial conditions were established by rinsing with 200 $\mu$M EDTA between experiments. (Panels a and b) original signals; (panels c and d) with the signal decay subtracted for clearer presentation. The lifetime of the signal in the 100-ms range is limited by the capacitance of the supporting film (~1.4 nF) and the 100-MΩ shunt resistor on the input of the amplifier but about 30% of the decay is faster due to ion leakage (10 ms in the absence and 30 ms in the presence of metal ions, respectively). For ease of comparison, all traces are normalized to equal amplitudes of the unresolved fast phase.

external donors, the membrane potential (and the photovoltage signal) persists for 100 ms or longer. Its decay at long times is mainly due to leakage of ions through the membrane of the fused chromatophores (Keller et al., unpublished results).

## RESULTS

*Effect of Metal Binding on Electrogenic Proton-Transfer Phases in R26 Chromatophores.* The traces in Figure 2 show on a logarithmic (panels a and b) and a linear (panels c and d) time scale the photovoltage response at pH 8 of *Rb. sphaeroides* R26 chromatophores without addition and after addition of 100 $\mu$M $Cd^{2+}$, $Zn^{2+}$, or $Ni^{2+}$, respectively. The data were taken on the first (panels a and c) and the second (panels b and d) flash of the same series of two flashes, separated by 0.5 s. The same sample was used for this series of experiments with a thorough rinsing with an EDTA solution between sets of experiments. In the control sample without metal, on the first flash, formation of $Q_B^-$ leads to a phase, B1, with small relative amplitude (at pH 8) with a rate of ~(400 $\mu$s)$^{-1}$. On the second flash, a phase, B2, with an amplitude significantly larger than that of B1 (about 15% relative to phase A) is observed (pH 8) with a rate of ~(300 $\mu$s)$^{-1}$.

Table 1: Exponential Time Constants and Relative Amplitudes of Electrogenic Proton Transfer Phases as Determined by a Best Fit to the Kinetic Traces in Figures 2 and 3[a]

| | first flash (B1) | | | | second flash (B2) | | | |
|---|---|---|---|---|---|---|---|---|
| | R26 | | 2× His mutant | | R26 | | 2× His mutant | |
| metal present | $a_1$ | $\tau_1$ | $a_1$ | $\tau_1$ | $a_2$ | $\tau_2$ | $a_2$ | $\tau_2$ |
| none | 4 | 0.4 | 9 | 0.24 | 15 | 0.3 | 21 | 0.48 |
| $Cd^{2+}$ | 11 | 1.0 | 11 | 0.4 | 13 | 1.2 | 16 | 1.1 |
| $Ni^{2+}$ | 12 | 1.5 | 10 | 0.37 | 13 | 1.1 | 19 | 0.7 |
| $Zn^{2+}$ | 18 | 2.5 | 13 | 2.6 | 17 | 2.3 | 16 | 2.8 |

[a] Values given are mean values from at least three different samples and the error given by the observed variation between different experiments is about ± 20% for both amplitudes (expressed as percentages) and time constants (given in ms). Both phases B1 and B2 could be well described by a single-exponential function in all cases. Conditions: pH 8, 25 °C, 100 mM KCl, and 100 $\mu$M metal ion where indicated.

The amplitude of the major fast phase due to $P^+Q_A^-$ formation phase (A) was not affected by the metals, whereas the relative amplitudes and rates of the slower phases (B1 and B2) were affected. The metals showed similar but not identical effects, which are best seen in the lower panels of Figure 2 (panels c and d) where the signal decay (caused by ion leakage) has been removed from the kinetic traces for clearer presentation. Upon addition of metal, B1 increased in amplitude (~ 3-fold) and became slower [$k \cong (1-2.5$ ms$)^{-1}$] (Table 1).

On the second flash, the addition of metal ions did not change the amplitude of phase A, whereas the kinetics of the phase attributed to proton transfer to $Q_B$ (B2) was slower [$k \cong (1-2$ ms$)^{-1}$]; the amplitude of B2 was essentially unaffected (Table 1). $Zn^{2+}$ had the largest effect of the metal ions tested with both the largest amplitude change and the slowest rate for both B1 and B2 (Table 1). Increasing the metal concentrations to 500 $\mu$M led to only a small ($Zn^{2+}$ or $Cd^{2+}$) or no ($Ni^{2+}$) additional decrease in the rates for B1 and B2 (data not shown). Evidence that $Zn^{2+}$ was also the strongest binding metal comes from experiments (data not shown) where 500 $\mu$M $Zn^{2+}$ was added to samples containing 100 $\mu$M $Cd^{2+}$ or 100 $\mu$M $Ni^{2+}$. The resultant kinetic transients were characteristic of bound $Zn^{2+}$. This is consistent with $Zn^{2+}$ binding displacement of $Cd^{2+}$ or $Ni^{2+}$. If 500 $\mu$M $Cd^{2+}$ or $Ni^{2+}$ were added to a sample containing 100 $\mu$M $Zn^{2+}$, the kinetics remained characteristic of bound $Zn^{2+}$. This shows that $Zn^{2+}$ is not displaced by the other metals.

Note that upon addition of metal, the difference between the relative amplitudes of B1 and B2 observed in R26 samples in the absence of metal disappears, and the rate constants become smaller. Control experiments with methylene blue, an efficient mediator for reoxidation of $Q_B^-$ (*56*), showed that the observed behavior was not due to the presence of $Q_B^-$ before excitation.

The effect of all metals was removed by the addition of a 2-fold molar excess of EDTA (not shown). It was found that metal binding was inefficient in samples that were not first rinsed with an EDTA solution. We attribute this to the

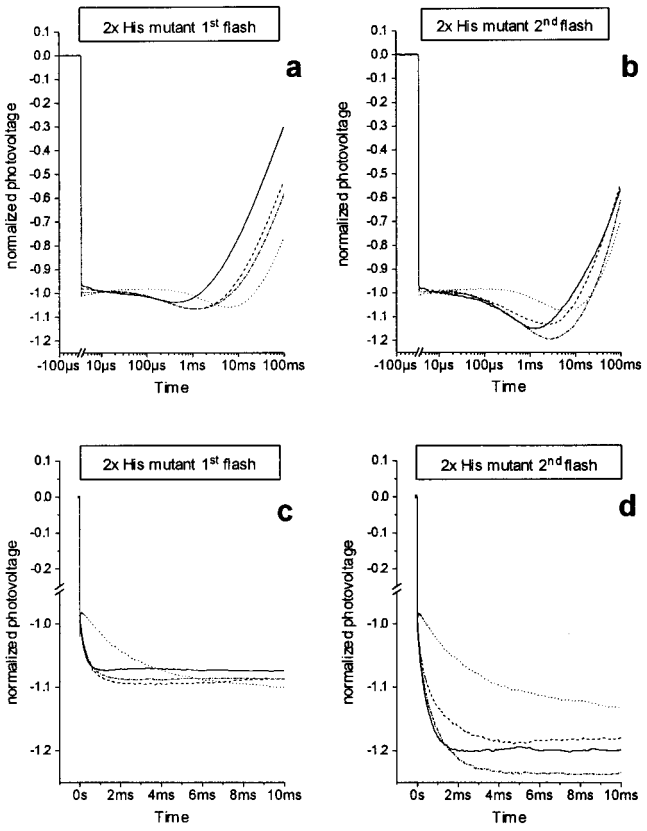


FIGURE 3: Effect of metal binding on photovoltage transients in chromatophores from the 2× histidine [HA(H126)/HA(H128)] mutant. (Panels a and c) first flash; (panels b and d) second flash of the same series of two flashes spaced 0.5 s. (—) no addition, (- - -) 100 $\mu$M $Cd^{2+}$, (•••) 100 $\mu$M $Zn^{2+}$, (•-•-•) 100 $\mu$M $Ni^{2+}$. 10 mM Hepes pH 8, 100 mM KCl, 1 mM ascorbate, and 2 $\mu$M PMS were present in all samples. The same sample of chromatophores fused to a lipid-coated gold/OM electrode was used for all experiments. Initial conditions were established by rinsing with 200 $\mu$M EDTA between experiments. For ease of comparison, the traces are normalized to equal amplitudes of the unresolved fast phase. (Panels a and b) original signals; (panels c and d) with the signal decay subtracted for clearer presentation as stated in Figure 2.

presence of residual $Ca^{2+}$, which was added to promote fusion of the chromatophores and which stays bound even after several rinses with $Ca^{2+}$-free solution. It is likely that $Ca^{2+}$ binds in a competitive manner to the same site as the other divalent metal ions studied in this work. When comparing traces recorded before and after EDTA washing or after readdition of 100 $\mu$M $Ca^{2+}$, it was noticed that $Ca^{2+}$ caused a slight decrease in the rate of B1 and B2 and an increase of the relative amplitude of B1 (data not shown). This observation is consistent with effects of ionic strength and $Ca^{2+}$ on B2 reported earlier (*51*, *54*). Whereas the major effect of salt concentration was interpreted in terms of a decrease in surface potential, the possibility of specific binding of cations to the protein had previously been suggested (*51*).

*Effect of Double Mutation His-H126Ala, His-H128Ala.* In isolated RCs, $Cd^{2+}$ and $Zn^{2+}$ bind to Asp-H124, His-H126, and His-H128 (*18*, *57*). To evaluate if the binding site of the metal ions in chromatophores is the same as in isolated RCs, we investigated a double mutant in which His-H126 and His-H128 were replaced by alanine (2× histidine mutant). Figure 3 shows the photovoltage response on the first and second flashes for chromatophores from this mutant. In the absence of metal ions (Figure 3, no addition), the 2× histidine mutant showed an ~2-fold larger amplitude for B1 (pH 8) than observed in R26 chromatophores with no change in the rate (Table 1). The amplitude of B2 was also increased (by ~40%) with a slight decrease in the rate (Table 1). Thus the main effect of the mutation is an increase in the amplitudes of both protonation phases, B1 and B2.

The addition of 100 $\mu$M $Cd^{2+}$ led to small changes in the electrogenic characteristics. B1 was slightly affected (by $\leq$50%), and the amplitude of B2 was decreased by ~ 25% and the rate decreased by ~2-fold (Table 1). Addition of 100 $\mu$M $Ni^{2+}$ had little effect (Table 1). However, higher concentrations of $Ni^{2+}$ induced similar effects as in the R26 sample (not shown). The addition of 100 $\mu$M $Zn^{2+}$ had about the same effect in the 2× histidine mutant as in the R26 sample, with an ~5−10-fold decrease in the rate of B1 and B2. For all metals added, the increase of the amplitude of B1 is accompanied by a decrease of the amplitude of B2,[2] leading to similar amplitudes of the phases B1 and B2. In addition, no significant effect of $Ca^{2+}$ was observed in the 2× histidine mutant chromatophores.

## DISCUSSION

In this study, we investigated the pathway for proton transfer from the cytoplasmic surface to the secondary electron acceptor $Q_B$ in chromatophores of *Rb. sphaeroides* by characterizing the effect on the electrogenic proton phases of modifications at the putative proton entry point. The entry point was modified by metal binding ($Zn^{2+}$, $Cd^{2+}$, and $Ni^{2+}$) or by replacement of two surface-exposed histidine residues with nonprotonatable alanine residues at the metal binding site (*18*). We measured the rate of formation and relative amplitudes of the electrogenic phases associated with proton transfer toward $Q_B$ after one or two flashes. An important aspect of this work is to investigate the similarities as well as possible differences in the function of the quinone acceptor complex between native membrane-bound RCs and isolated RCs in which inhibition of proton transfer by metal ions was first reported (*16*, *17*).

The interpretation of photovoltage transients involves two aspects, rates and amplitudes. The rates reflect the time course of electrical charge movements, which in our case involve protons. The amplitudes observed in photovoltage measurements result from two contributing factors, the amount (stoichiometry) of charges transferred and the dielectrically weighted transmembrane distance over which the transfers occur. Below, we provide an explanation of how the electrogenic proton-transfer phases could be modified by the binding of metal ions and by the 2× histidine mutation in the light of the different proposed proton pathways.

[2] An exception is the binding of $Zn^{2+}$ in R26 chromatophores, which led to an increase in the amplitude of both B1 and B2. For completeness, it should be mentioned that addition of metal ions has a secondary effect. It causes a slowdown of the decay phase of the photovoltage signal. This is most clearly seen in the traces of Figure 3 (panels a and b). In these experiments with the gold/OM electrode the capacitance of the system is much higher than with the Mylar film, leading to a slower apparent decay (the shunt resistor $R$ was 100 M$\Omega$; see Figure 1). Under these conditions, the recovery of the potential change at long times is exclusively limited by ion leakage through the chromatophore membranes. A likely explanation for the longer lifetime of the flash-induced potential in the presence of metal ions is that the latter block ion leakage through the chromatophore membrane.

*Comparison to Previous Measurements.* The general features of electrogenicity observed in this work on R26 samples (Figure 2, Table 1) agree well with data reported in the literature (see Scheme 1). In particular, it has been shown that the relative amplitude of the phase B1 on the first flash is small at neutral pH but increases at acidic and alkaline pH (not shown, see refs *49* and *52*). This phase has been attributed to substoichiometric proton uptake and electrogenic protonation of residues whose p$K_a$ value is shifted due to electrostatic interaction with the charge on $Q_B^-$.[3] It is worth noting that a phase reported in RCs oriented on a Teflon film with inverse electrogenicity and kinetics reflecting electron transfer to $Q_B$ (*58*) is not observed in chromatophores. It had been proposed that this phase is due to a conformational change related with gating of the electron transfer. If a similar reaction exists in chromatophores, it might be electrically silent. Upon the second flash, the phase B2 has an amplitude of 15−20% relative to phase A and is attributed to proton uptake and transfer of two protons to $Q_B^-$ to form the ubiquinol $Q_BH_2$.

In most previous studies, the phases related to proton uptake upon $Q_B$ reduction (B1 and B2) have been analyzed after subtraction of traces recorded after addition of $Q_B$ inhibitors, like atrazine or terbutryn, to subtract eventual contributions not related to $Q_B$ function. In this study, we choose not to use subtraction of traces taken in the presence of an inhibitor but rather to analyze the traces directly. The rationale for this is the functional linkage between the $Q_A$ and $Q_B$ site (*59*, *60*, and references therein). In view of the coupling of protonation events occurring upon $Q_A^-$ or $Q_B^-$ formation, subtraction of the two traces may lead to systematic errors. There are indications that the proton uptake upon $Q_A^-$ formation (as detectable in the presence of inhibitors) is mainly by residues near $Q_B$ (*21*, *61*−*63*). To our knowledge, the electrogenicity of proton uptake in the state $Q_A^-$ has not been investigated so far. As it is likely that proton uptake in the states $Q_A^-$ and $Q_B^-$ is not additive (the protons taken up in the state $Q_A^-$ constitute part of the proton uptake upon $Q_B^-$ formation), the amount of proton uptake in the state $Q_B^-$ will be underestimated by subtracting the part of proton uptake occurring in the state $Q_A^-$.

*Metal Binding Site.* In RC crystals, $Cd^{2+}$ and $Zn^{2+}$ bind to His-H126, His-H128, and Asp-H124 whereas $Ni^{2+}$ binds to Asp-M17 and His-H126 (*18*). To test whether this is the binding site in chromatophores, a double mutant was constructed in which His-H126 and His-H128 were replaced with Ala [2× histidine mutant, (*57*)]. The addition of 100 $\mu$M $Ni^{2+}$ or $Cd^{2+}$ had little effect on the electrogenic phases. However, upon addition of greater amount of metal ions, both the kinetics and the amplitudes became more similar to those found in the R26 chromatophores with the metal. The most straightforward explanation would be a decreased binding affinity for $Ni^{2+}$ or $Cd^{2+}$ in the 2× histidine mutant in agreement with observations in isolated RCs (*57*). This confirms that the binding site of these metal ions (in the R26 system) is the same in chromatophores and isolated RCs. In contrast, addition of 100 $\mu$M $Zn^{2+}$ to chromatophores of the 2× histidine mutant does result in a slower rate for B1 and B2. A possible reason for the $Zn^{2+}$ effect in the double histidine mutant is that $Zn^{2+}$ alternatively binds to the now exposed acid groups of Asp-M17, Asp-L210, and Asp-H124. If this is the case then it must be concluded that binding of $Cd^{2+}$ or $Ni^{2+}$ to these aspartic acid residues is significantly weaker.

*Proton Entry Point.* Upon metal binding to R26 chromatophores, the rate of the electrogenic phase B1 was decreased ∼3−5-fold and the amplitude increased ∼3−4-fold (Table 1). With respect to kinetics, we note that proton movements detected by photovoltage need not have the same kinetics as electron transfer to $Q_B$ ($k_{AB}^{(1)}$). In a recent study of electrochromism in chromatophores of *Rb. sphaeroides*, several kinetic phases were observed. The faster phases were assigned to electron transfer and the slowest phase to proton uptake (*27*). In isolated RCs, the kinetic phases were more similar in rate.

In isolated RCs with bound $Zn^{2+}$, $k_{AB}^{(1)}$ was decreased by ∼10-fold as compared to R26 RCs (*16*, *17*). The rate constants of B1 determined in chromatophores in the presence of metal ions $(1.0-2.5\ ms)^{-1}$ compare reasonably well with the rate of $k_{AB}^{(1)}$ of $(1.4\ ms)^{-1}$ found in isolated RCs. This is taken to indicate that upon metal binding, both electron transfer (as measured by $k_{AB}^{(1)}$) and proton transfer (as measured by photovoltage kinetics) become slow and kinetically correlated. The decrease in the observed rate was attributed to a slowing down of a conformationally gated step that limits electron transfer to $Q_B$ due to its similar kinetic behavior to RCs at 2 °C in the absence of $Zn^{2+}$ (*16*). Paddock et al. (*17*) showed that $Cd^{2+}$ had a similar effect on $k_{AB}^{(1)}$ and favored a similar interpretation, although alternative explanations such as hindered uptake and/or redistribution of protons that stabilize the semiquinone were not excluded. The importance of protein rearrangements for electron transfer to $Q_B$, as well as the necessity of proton uptake for stabilization of the state $Q_B^-$, were also noted in recent electrostatic calculations (*21*). There is also experimental evidence that the rate-limiting step of $k_{AB}^{(1)}$ is conformationally gated (*64*) and that proton rearrangement controls the "gating step" (*53*). Recently, a mechanistic model based on conformationally controlled p*K*-switching has been proposed that provides a link between these two mechanisms (*55*, *65*). In this model, movement of $Q_B$ from a distal to a proximal binding position is connected to a change in the protonation state of Glu-L212.

The electrogenic phase B2 on the second flash is directly related to the supply of two protons to $Q_B$ (i.e., B2 is the sum of B2a and B2b, Scheme 1). The first proton is kinetically coupled to the transfer of the second electron to $Q_B$ (B2a, Scheme 1), occurring with rate constant $k_{AB}^{(2)}$. This coupling of electron and proton transfer holds even in the presence of metals, where it has been shown that transfer of the first proton becomes rate-limiting (*17*). The second proton after formation of $Q_BH^-$ must be transferred rapidly (B2b, Scheme 1), as B2 is not biphasic in R26 chromatophores or in the presence of metal ions. However, B2 displayed biphasic kinetics at lower temperature (*54*). The two phases were attributed to the transfer to $Q_B$ of the first and second proton, respectively, and a model was proposed in which unbinding of $Q_BH^-$ is the rate-limiting step for the second

[3] At temperatures below 15 °C, this phase was reported to split into two components with different activation energy (*53*). The two components were attributed to two conformations of the oxidized ubiquinone at the $Q_B$ site, differing by the presence or absence of a hydrogen bond between Glu-L212 and one of the methoxy groups of $Q_B$.

protonation of $Q_B$ (*55*, *65*). That the second proton contributes to B2 has also been shown by the diminished amplitude in a Glu-L212 → Gln mutant in which the transfer of the second proton is blocked (*66*). Binding of $Zn^{2+}$ or $Cd^{2+}$ decreased $k_{AB}^{(2)}$ in isolated RC 10-fold or 20-fold, respectively (*17*). The fact that $k_{AB}^{(1)}$ and $k_{AB}^{(2)}$ are decreased by a similar factor suggests that metal binding inhibits proton transfer or uptake on the first and second flash by a common mechanism. In agreement with the optical kinetic measurements in isolated RCs, our photovoltage measurements show that in R26 chromatophores, the addition of metal ions has similar effects on the B1 and B2 phases[4] (Figure 2). This result suggests that in the presence of metal ions, the same reaction step is rate-limiting for B1 and B2, namely, proton uptake or proton rearrangement.

We are left with the question by which mechanism metal binding decreases the rate of proton delivery toward $Q_B$. Two contributions, which are not exclusive, may be considered. First, one or more of the residues involved in metal binding (His-H126, His-H128, Asp-H124, and Asp-M17) might be essential for proton uptake. The binding of the metal to the residue prevents it from facilitating proton uptake. Second, the binding of the metal ion diminishes the effective concentration of protons near the entry point (electrostatic repulsion). The small effect of the His-H126/His-H128 mutation on the kinetics of proton transfer observed in the present work seems to exclude His-H126/His-H128 as essential for proton uptake at pH 8. However, it is possible that in this mutant the substitution of the His side chains with smaller Ala residues results in other protonatable groups, such as Asp-L210, becoming solvent-accessible, allowing them to substitute for these His residues in proton uptake. In this case, the absence of a decrease of the kinetics in the 2× histidine mutant does not necessarily disqualify these His side chains as proton acceptors in the R26 system. Replacements of these His residues with structurally more conservative amino acids (e.g., Phe) could help to clarify this point. The dominant contribution to the decrease in the rate of proton uptake comes probably from electrostatic repulsion of protons near the entry point by the bound metal ion, but it cannot be excluded that metal binding has less direct effects, for example, on the functional organization (e.g., $H^+$-bonding energies, local dynamics) of the hydrogen-bonded network connecting the metal binding site residues to the $Q_B$ site. Although normally it is not expected that proton conduction within this proton well is rate-limiting, an unfavorable intermediate may create a barrier slowing down proton conduction along the network. Nevertheless, the binding of a metal ion to His-H126 and His-H128 or Asp-M17 inhibits proton uptake and identifies this region as the entry point for the protons.

*Internal Proton Rearrangement.* Below we will discuss possible mechanisms by which metal binding and the mutation can result in an increase in the relative amplitude of B1. Two factors can contribute to an increase of the photovoltage amplitude: an increase in proton uptake stoichiometry or an increase in the dielectrically weighted transmembrane distance for the proton-transfer event.[5] The metal binding site is close to the entry point of one of the proposed proton pathways from the cytoplasmic surface to $Q_B$ (P3) (Figure 4). With a bound $Cd^{2+}$, mutations of residues in path P3 (Asp-M17 and Asp-L210) led to a decrease in the rate of transfer of the second proton in isolated RCs by 1 order of magnitude (*68*). This indicates that alternative pathways are much less efficient and are not competitive even when proton uptake through P3 is slowed by metal binding. Assuming that the same situation holds for RCs bound in the membrane of the chromatophores, the binding of the metal ion most likely increases the stoichiometry of proton uptake on the first flash.[6] Correspondingly, a decrease in the amplitude of B2 is observed upon metal binding (except for $Zn^{2+}$ in R26 samples, Table 1). The similar amplitudes of B1 and B2 in the presence of metal ions suggest that under these conditions about one proton is transferred into the $Q_B$ site on the first flash and one proton on the second flash.

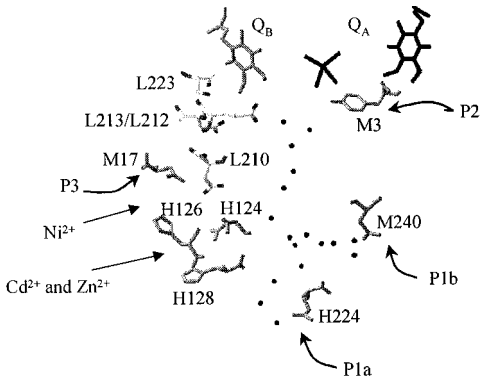


FIGURE 4: Part of the RC structure showing the region between the metal binding site and $Q_B$. Positions of metal ions (*18*) and entry points of proton pathways proposed by Abresch et al. (*14*) are indicated by arrows. Points represent water molecules involved in pathway P1a and P1b. Coordinates were taken from dark RC structure 1AIJ except for $Q_B^-$, the coordinates of which were taken from the light RC structure 1AIG (*74*).

In principle, proton uptake compensates for the thermodynamic penalty for introduction of a negative charge. Uptake of a full proton upon one electron reduction is not uncommon. For example, one model for the catalytic cycle in cytochrome *c* oxidase is based on an electroneutrality principle where each electron transferred to a membrane-embedded electron acceptor is stabilized by uptake of one proton (*69*, *70*). Rather, the question arises why, in the R26 system, proton uptake (and electrogenicity of proton transfer)

[4] The faster absolute rate of B2 in chromatophores as compared to $k_{AB}(2)$ in isolated RCs could be due to a transient confinement of protons at the membrane surface (*67*), an effect which, in the R26 system, is especially visible on the second flash where a larger fraction of protons is taken up from solution.

[5] The addition of metal ions did not increase the occupancy of the $Q_B$ site as evident from the unmodified amplitude of phase A on the second flash.

[6] The increase in amplitude of the phase B1 (by about a factor of 3 to 4) induced by metal binding cannot be explained by activation of another pathway with an increased transmembrane distance for proton transfer. Although one of the proposed pathways (P1a) extends over a larger transmembrane distance than the path P3 (Figure 4), a proton transferred through P1a would lead to a small, if any, increase in the observed amplitude. This is due to the high effective dielectric constant expected in this part of subunit H, which is well outside the membrane dielectric and exposed to the aqueous solution. In other words, protons are taken up from an (quasi)equipotential surface. Transfer of the protons through the extramembranous part of the protein will not contribute significantly to the membrane potential.

is unbalanced on the first and second flash. Typical values from proton uptake measurements indicate at pH 8 uptake of ~0.4 $H^+$ on the first and ~1.6 $H^+$ on the second flash (see, for example, ref *71*), and typical values for the relative amplitudes of photovoltage phases B1 and B2 are ~4% and 15−20%, respectively (*49*, *51*−*55*). It is commonly accepted that two key residues, Glu-L212 and Asp-L213, control proton uptake and electrogenicity on the first flash (*13*, *52*, *61*, *66*, *72*). Replacement of Glu-L212 with Gln eliminates proton uptake at high pH whereas replacement of Asp-L213 with Asn eliminates proton uptake at low pH. There is strong evidence from infrared studies that Glu-L212 increases its protonation state upon $Q_B$ reduction at neutral pH and shows a nonclassic titration behavior (*24*, *25*). Strong electrostatic interactions between titrating acids can lead to complicated titration behaviors and make it difficult to attribute observed p$K_a$ values to any one carboxylic acid. It is probably more appropriate to talk about (upper and lower) apparent p$K_a$ values of the Glu-L212/Asp-L213 couple keeping in mind that other residues of the cluster might contribute to the titration behavior.

To explain the increased amplitude of B1, we propose the following model. In the R26 system, an internal proton donor exists, which delivers about one proton to the (Glu-L212/Asp-L213) cluster near $Q_B$ after the first flash but that is not, or only partially, reprotonated by $H^+$ uptake from solution. Full reprotonation of this residue occurs only after the second flash. Binding of a metal ion inhibits the function of this residue as internal proton source provoking uptake of ~1 $H^+$ from solution upon formation of $Q_B^-$.

The increase in the amplitude of phase B1 observed in the 2× histidine mutant could indicate that these His residues are a proton source. However, this is unlikely for two reasons. First, it is difficult to explain why proton donors at the protein surface, far from $Q_B$, would not be reprotonated rapidly as electrostatic interaction with $Q_B^-$ is expected to be weak. Second, the difference in electrogenicity for transfer of protons to the $Q_B$ site either from these His residues or from solution is expected to be small. This is in contradiction with the large increase in electrogenicity of the phase B1 observed upon metal binding.

According to the relative photovoltage amplitudes, the putative internal proton source must be located closer to $Q_B$, on the pathway connecting the metal binding site and the $Q_B$ site. An obvious candidate for a residue fulfilling this condition is Asp-L210, which is situated between the (Glu-L212/Asp-L213) cluster and the metal binding site (Figure 4). Calculations of side chain ionization and conformation (*21*) provide insight into the details of protonation events accompanying the first reduction of $Q_B$. According to these simulations, the strongly coupled acids Glu-L212 and Asp-L213 always share one proton in the state $Q_B$ and both are protonated in the state $Q_B^-$. Between pH 7 and 9 Asp-L210 is the proton donor for the (Glu-L212/Asp-L213) cluster. The protonation state of Asp-L210 is controlled by interaction with the (Asp-L213/Glu-L212) cluster, and it is energetically unfavorable to have all three acids ionized simultaneously. In the $Q_B$ state, the protonated Asp-L210 is stabilized by interaction with the ionized Asp-L213. Upon formation of $Q_B^-$, Asp-L213 becomes protonated and Asp-L210 becomes ionized (i.e., its p$K_a$ is shifted down due to the loss of the nearby ionized acid). In this way, Asp-L210 can be considered as an internal proton source, which upon $Q_B^-$ formation delivers a proton to (Asp-L213/Glu-L212) without being (fully) reprotonated. According to the calculations, the proton is transferred predominantly to Asp-L213. Protonation of Glu-L212 had also been proposed connected with movement of $Q_B$ from a distal to a proximal binding position and formation of a hydrogen bond between Glu-L212 and a methoxy group of $Q_B$ in a fraction of RC (*53*, *55*, *65*). These ideas agree with molecular dynamics simulations, which suggest that $Q_B$ occupies the distal position until both Asp-L213 and Glu-L212 are protonated (*73*). However, for the purpose of the discussion of the photovoltage data, it is not important whether the proton is transferred to Glu-L212 or Asp-L213, due to the similar transmembrane location of these two residues.

As pointed out by Alexov and Gunner (*21*), increased proton uptake above pH 9 is largely a result of the inability of Asp-L210 to be protonated in the ground state so that much of the proton transfer to Asp-L213 now comes from solution. Indeed, from a phenomenological point of view, the changes in the amplitudes of phases B1 and B2 induced by metal binding at pH 8 observed in the present work are very reminiscent of the effect of an increase in pH in R26 samples (not shown, see e.g., *49*). It is therefore tempting to explain the effect of metal binding on the amplitudes by a shift to lower pH of an apparent p$K_a$ of a residue that controls proton transfer. In the context of our working model, the bound metal ion stabilizes the ionized state of Asp-L210. As a consequence, protonation of (Glu-L212/Asp-L213) requires proton uptake from solution. This involves proton translocation over twice the transmembrane distance than occurs for internal proton transfer from Asp-L210 to Glu-L212 or Asp-L213. This model predicts the increase in the amplitude of B1 that is experimentally observed. Although the tentative identification of Asp-L210 as the internal proton source is consistent with recent calculations (*21*), it cannot be excluded that other nearby carboxylic acids or water molecules are involved.

Since metal binding induces no major structural change in the $Q_B$ pocket (*18*), the most likely explanation for the effect of binding of a metal ion is electrostatic stabilization of the ionized state of an internal carboxylic acid (e.g., Asp-L210). The distance between water w72 (which is bound to His-H126 and His-H128 and which is displaced by $Cd^{2+}$ and $Zn^{2+}$) and the carboxyl groups of the side chain of Asp-L210 is about 7−8 Å. Assuming a single charge on the metal and a dielectric constant of ~20, the interaction energy between the bound metal ion and Asp-L210 is estimated to be ~2 kcal/mol. This interaction decreases the p$K_a$ of Asp-L210 by 1.5 units, which might be sufficient to explain ionization of this residue in the state $Q_B$ at neutral pH.[7] Thus, in our model, the metal ion shifts the p$K_a$ of Asp-L210 to a lower value eliminating it as a proton source.

[7] Interactions with other titrating groups and nonelectrostatic interactions between the metal ion and Asp-L210 may also contribute. In particular, the binding of the metal ion could perturb a water molecule (w74) involved in hydrogen bonds with both Asp-L210 and Asp-H124, the latter being one of the three residues coordinating $Cd^{2+}$ or $Zn^{2+}$ (*18*). In the case of $Ni^{2+}$, this water molecule could even be a direct ligand to the metal. Slight changes in the water position could affect the hydrogen bond strength, which is another mechanism by which metal binding could affect the protonation state of Asp-L210.

The working model presented above predicts that the inhibition of Asp-L210 as internal proton source should disappear at a sufficiently low pH, where this residue is protonated in the ground-state despite interaction with the metal ion. It also predicts that at pH 8 there would be increased proton uptake from solution on the first flash in the presence of metal ions, which could be verified by measurements of proton uptake with indicator dyes.

## CONCLUSIONS

(i) The effect of metal binding ($Zn^{2+}$, $Cd^{2+}$, $Ni^{2+}$) in chromatophores is qualitatively similar to the effect observed in isolated RCs, suggesting that the cause of the kinetic effects is the same in chromatophores and in isolated RCs.

(ii) The decreased binding of $Cd^{2+}$ and $Ni^{2+}$ in the 2× histidine mutant [HA(H126)/HA(H128)] indicates that these binding sites in chromatophores correspond to the binding sites determined by X-ray crystallography.

(iii) The two above conclusions suggest that in chromatophores, as in isolated RCs, there exists a unique proton entry point (close to Asp-M17, His-H126, and His-H128) for proton uptake associated with $Q_B$ reduction.

(iv) The increase in the amplitude of the electrogenicity of proton transfer on the first flash upon binding metal is attributed to an increase in the stoichiometry of proton uptake from solution caused by elimination upon metal binding of internal proton rearrangements that stabilize $Q_B^-$. The similar amplitudes on the first and second flash with bound metal ion indicate that one proton is taken up on both electron transfers to $Q_B$.

## ACKNOWLEDGMENT

We thank Profs. Christian Bourdillon and Jean-Marc Laval for valuable help with the gold/OM electrode system and Yann Riou for repeated and timely preparation of gold/OM electrodes, Drs. Eliane Nabedryk, Mel Okamura, and George Feher for helpful discussions, Sandra Andrianambinintsoa for experimental help, and Philippe Lebel, Christian Schneider, and Yves Penn for their ingenious work concerning the development of the hardware and software for the data acquisition system with programmable time base. We also gratefully acknowledge Dr. Armen Mulkidjanian for valuable discussions and communication of results prior to publication.

## REFERENCES

1. Shinkarev, V. P., and Wraight, C. A. (1993) in *The Photosynthetic Reaction Center* (Deisenhofer, J., and Norris, J. R., Eds.) Vol. I, pp 193−255, Academic Press, New York.
2. Okamura, M. Y., and Feher, G. (1995) in *Anoxygenic Photosynthetic Bacteria* (Blankenship, R. E., Madigan, M. T., and Bauer, C. E., Eds.) pp 577−594, Kluwer Academic Publishers, Dordrecht.
3. Blankenship, R. E., Madigan, M. T., and Bauer, C. E., Eds. (1995) *Anoxygenic Photosynthetic Bacteria*, Kluwer Academic Publishers, Dordrecht.
4. Maroti, P., and Wraight, C. A. (1988) *Biochim. Biophys. Acta 934*, 329−347.
5. McPherson, P. H., Okamura, M. Y., and Feher, G. (1988) *Biochim. Biophys. Acta 934*, 348−368.
6. Kleinfeld, D., Okamura, M. Y., and Feher, G. (1984) *Biochim. Biophys. Acta 766*, 126−140.
7. Kleinfeld, D., Okamura, M. Y., and Feher, G. (1985) *Biochim. Biophys. Acta 809*, 291−310.
8. Graige, M. S., Paddock, M. L., Bruce, J. M., Feher, G., and Okamura, M. Y. (1996) *J. Am. Chem. Soc. 118*, 9005−9016.
9. Graige, M. S., Paddock, M. L., Feher, G., and Okamura, M. Y. (1999) *Biochemistry 38*, 11465−11473.
10. Nagle, J. F., and Tristram-Nagle, S. (1983) *J. Membrane Biol. 74*, 1−4.
11. Paddock, M. L., Rongey, S. H., Feher, G., and Okamura, M. Y. (1989) *Proc. Natl. Acad. Sci. U.S.A. 86*, 6602−6606.
12. Takahashi, E., and Wraight, C. A. (1990) *Biochim. Biophys. Acta 1020*, 107−111.
13. Takahashi, E., and Wraight, C. A. (1992) *Biochemistry 31*, 855−866.
14. Abresch, E. C., Paddock, M. L., Stowell, M. H. B., McPhilips, T. M., Axelrod, H. L., Soltis, S. M., Rees, D. C., Okamura, M. Y., and Feher, G. (1998) *Photosynth. Res. 55*, 119−125.
15. Ermler, U., Fritzsch, G., Buchanan, S. K., and Michel, H. (1994) *Structure 2*, 925−936.
16. Utschig, L. M., Ohigashi, Y., Thurnauer, M. C., and Tiede, D. M. (1998) *Biochemistry 37*, 8278−8281.
17. Paddock, M. L., Graige, M. S., Feher, G., and Okamura, M. Y. (1999) *Proc. Natl. Acad. Sci. U.S.A. 96*, 6183−6188.
18. Axelrod, H. L., Abresch, E. C., Paddock, M. L., Okamura, M. Y., and Feher, G. (2000) *Proc. Natl. Acad. Sci. U.S.A. 97*, 1542−1547.
19. Maroti, P., Hanson, D. K., Baciou, L., Schiffer, M., and Sebban, P. (1994) *Proc. Natl. Acad. Sci. U.S.A. 91*, 5617−5621.
20. Takahashi, E., and Wraight, C. A. (1996) *Proc. Natl. Acad. Sci. U.S.A. 93*, 2640−2645.
21. Alexov, E. G., and Gunner, M. R. (1999) *Biochemistry 38*, 8253−8270.
22. Lancaster, C. R. D., Michel, H., Honig, B., and Gunner, M. R. (1996) *Biophys. J. 70*, 2469−2492.
23. Rabenstein, B., Ullmann, G. M., and Knapp, E.-W. (1998) *Biochemistry 37*, 2488−2495.
24. Nabedryk, E., Breton, J., Hienerwadel, R., Fogel, C., Mäntele, W., Paddock, M. L., and Okamura, M. Y. (1995) *Biochemistry 34*, 14722−14732.
25. Hienerwadel, R., Grzybek, S., Fogel, C., Kreutz, W., Okamura, M. Y., Paddock, M. L., Breton, J., Nabedryk, E., and Mäntele, W. (1995) *Biochemistry 34*, 2832−2843.
26. Vermeglio, A. (1982) in *Function of quinones in energy conserving systems* (Trumpower, B. L., Ed.) pp 169−180, Academic Press, New York.
27. Tiede, D. M., Utschig, L., Hanson, D. K., and Gallo, D. M. (1998) *Photosynth. Res. 55*, 267−273.
28. Lavergne, J., Matthews, C., and Ginet, N. (1999) *Biochemistry 38*, 4542−4552.
29. Tiede, D. M., Vazquez, J., Cordova, J., and Marone, P. A. (1996) *Biochemistry 35*, 10763−10775.
30. Lancaster, C. R. D., and Michel, H. (1997) *Structure 5*, 1339−1359.
31. Warncke, K., Gunner, M. R., Braun, B. S., Gu, L., Yu, C.-A., Bruce, J. M., and Dutton, P. L. (1994) *Biochemistry 33*, 7830−7841.
32. Barz, W. P., Verméglio, A., Francia, F., Venturoli, G., Melandri, B. A., and Oesterhelt, D. (1995) *Biochemistry 34*, 15248−15258.
33. Lilburn, T. G., Recchia, P. A., Parkes-Loach, P. S., Loach, P. A., Prince, R. C., and Beatty, J. T. (1998) in *Photosynthesis: Mechanisms and Effects* (Garab, G., Ed.) Vol. IV, pp 2841−2845, Kluwer, Dordrecht.
34. Semenov, A. Y., Mamedov, M. D., Shinkarev, V. P., Verkhovsky, M. I., and Zakharova, N. I. (1990) in *Molecular Biology of Membrane-Bound Complexes in Phototrophic Bacteria* (Drews, G., and Dawes, E. A., Eds.) pp 329−335, Plenum Press, New York.
35. Semenov, A. Y. (1991) in *Sov. Sci. Rev. Section D*, (Skulachev, V. P., Ed.) Vol. 10, pp 45−75, Harwood Acad. Publishers, UK.
36. Donohue, T. J., Hoger, J. H., and Kaplan, S. (1986) *J. Bacteriol. 168*, 953−961.
37. Keen, N. T., Tamaki, S., Kobayashi, D., and Trollinger, D. (1988) *Gene 70*, 191−197.

38. Lee, J. K., and Kaplan, S. (1995) *J. Biol. Chem. 270*, 20453−20458.
39. Chen, X.-Y., Yurkov, V., Paddock, M. L., Okamura, M. Y., and Beatty, J. T. (1998) *Photosyn. Res. 55*, 369−373.
40. Clayton, R. K., and Wang, R. T. (1971) *Methods Enzymol. 23*, 697−703.
41. Dracheva, S. M., Drachev, L. A., Konstantinov, A. A., Semenov, A. Y., Skulachev, V. P., Arutjunjan, A. M., Shuvalov, V. A., and Zaberezhnaya, S. M. (1988) *Eur. J. Biochem. 171*, 253−264.
42. Moltke, S., and Heyn, M. P. (1995) *Biophys. J. 69*, 2066−2073.
43. Drachev, L. A., Dracheva, S. M., Samuilov, V. D., Semenov, A. Y., and Skulachev, V. P. (1984) *Biochim. Biophys. Acta 767*, 257−262.
44. Brzezinski, P., Messinger, A., Blatt, Y., and Kleinfeld, D. (1998) *J. Membrane Biol. 165*, 213−225.
45. McComb, J. C., Stein, R. R., and Wraight, C. A. (1990) *Biochim. Biophys. Acta 1015*, 156−171.
46. Drachev, L. A., Kaminskaya, O. P., Konstantinov, A. A., Semenov, A. Y., and Skulachev, V. P. (1985) *FEBS Lett. 189*, 45−49.
47. Drachev, L. A., Kaurov, B. S., Mamedov, M. D., Mulkidjanian, A. Y., Semenov, A. Y., Shinkarev, V. P., Skulachev, V. P., and Verkhovsky, M. I. (1989) *Biochim. Biophys. Acta 973*, 189−197.
48. Shinkarev, V. P., Brunner, R., White, J. O., and Wraight, C. A. (1999) *FEBS Lett. 452*, 223−227.
49. Drachev, L. A., Mamedov, M. D., Mulkidjanian, A. Y., Semenov, A. Y., Shinkarev, V. P., and Verkhovsky, M. I. (1990) *FEBS Lett. 259*, 324−326.
50. Dobek, A., Deprez, J., Paillotin, G., Leibl, W., Trissl, H.-W., and Breton, J. (1990) *Biochim. Biophys. Acta 1015*, 313−321.
51. Shinkarev, V. P., Drachev, L. A., Mamedov, M. D., Mulkidjanian, A. J., Semenov, A. Y., and Verkhovsky, M. I. (1993) *Biochim. Biophys. Acta 1144*, 285−294.
52. Brzezinski, P., Paddock, M. L., Okamura, M. Y., and Feher, G. (1997) *Biochim. Biophys. Acta 1321*, 149−156.
53. Gopta, O. A., Bloch, D. A., Cherepanov, D. A., and Mulkidjanian, A. Y. (1997) *FEBS Lett. 412*, 490−494.
54. Gopta, O. A., Cherepanov, D. A., Mulkidjanian, A. Y., Semenov, A. Y., and Bloch, D. A. (1998) *Photosynth. Res. 55*, 309−316.
55. Cherepanov, D. A., Bibikov, S. I., Bibikova, M. V., Bloch, D. A., Drachev, L. A., Gopta, O. A., Oesterhelt, D., Semenov, A. Y., and Mulkidjanian, A. Y. (2000) *Biochim. Biophys. Acta 1459*, 10−34.
56. Mulkidjanian, A. Y., Shinkarev, V. P., Verkhovsky, M. I., and Kaurov, B. S. (1986) *Biochim. Biophys. Acta 849*, 150−161.
57. Beatty, J. T., Paddock, M. L., Feher, G., and Okamura, M. (2000) *Biophys J. 78*, 339A.
58. Brzezinski, P., Okamura, M. Y., and Feher, G. (1992) in *The Photosynthetic Bacterial Reaction Center II* (Breton, J., and Verméglio, A., Eds.) pp 321−330, Plenum Press, New York.
59. Maroti, P., Hanson, D. K., Schiffer, M., and Sebban, P. (1995) *Nat. Struct. Biol. 2*, 1057−1059.
60. Wraight, C. A. (1998) in *Photosynthesis: Mechanisms and Effects* (Garab, G., Ed.) Vol. II, pp 693−698, Kluwer, Dordrecht.
61. Miksovska, J., Maroti, P., Tandori, J., Schiffer, M., Hanson, D. K., and Sebban, P. (1996) *Biochemistry 35*, 15411−15417.
62. Kalman, L., Sebban, P., Hanson, D. K., Schiffer, M., and Maroti, P. (1998) *Biochim. Biophys. Acta 1365*, 513−521.
63. Miksovska, J., Schiffer, M., Hanson, D. K., and Sebban, P. (1999) *Proc. Natl. Acad. Sci. U.S.A. 96*, 14348−14353.
64. Graige, M. S., Feher, G., and Okamura, M. Y. (1998) *Proc. Natl. Acad. Sci. U.S.A. 95*, 11679−11684.
65. Mulkidjanian, A. Y. (1999) *FEBS Lett. 463*, 199−204.
66. Shinkarev, V. P., Takahashi, E., and Wraight, C. A. (1993) *Biochim. Biophys. Acta 1142*, 214−216.
67. Gopta, O. A., Cherepanov, D. A., Junge, W., and Mulkidjanian, A. Y. (1999) *Proc. Natl. Acad. Sci. U.S.A. 96*, 13159−13164.
68. Paddock, M. L., Feher, G., and Okamura, M. Y. (2000) *Proc. Natl. Acad. Sci. U.S.A. 97*, 1548−1553.
69. Mitchell, R., and Rich, P. R. (1994) *Biochim. Biophys. Acta 1186*, 19−26.
70. Michel, H. (1999) *Biochemistry 38*, 15129−15140.
71. McPherson, P. H., Okamura, M. Y., and Feher, G. (1993) *Biochim. Biophys. Acta 1044*, 309−324.
72. McPherson, P. H., Schönfeld, M., Paddock, M. L., Okamura, M. Y., and Feher, G. (1994) *Biochemistry 33*, 1181−1193.
73. Grafton, A. K., and Wheeler, R. A. (1999) *J. Phys. Chem. 103*, 5380−5387.
74. Stowell, M. H. B., McPhillips, T. M., Rees, D. C., Soltis, S. M., Abresch, E., and Feher, G. (1997) *Science 276*, 812−816.

BI001286N